Theory of the Crystallization of Hard Polymeric Chains in an Orienting Field

Nazar Sushko,*,† Paul van der Schoot, and M. A. J. Michels

Polymer Physics Group, Department of Applied Physics and Dutch Polymer Institute, Technische Universiteit Eindhoven, P.O. Box 513, 5600 MB Eindhoven, The Netherlands

Received June 25, 2003; Revised Manuscript Received October 29, 2003

ABSTRACT: We apply a recently proposed density functional theory (DFT) for hard polymeric chains to study the influence of a quadrupolar orienting field on the freezing of model polymers. We find that a "disorienting" field, mimicking elongational flow, promotes crystallization, while an "orienting" field, which corresponds to longitudinal shear flow, destabilizes the crystal phase. We also investigate the relative stability of two close-packed crystal lattice types, face-centered cubic and hexagonal close-packed. Geometrical effects, such as the orientation of the field with respect to the main axes of the crystal, play an important role in stabilizing one crystal type over another.

1. Introduction

High-tensile polymeric materials are important in many industrial applications,[1] and the problem of producing such materials based on highly oriented samples is of great interest in the field of polymer technology and processing. Oriented polymeric materials can be obtained by different methods from the solid phase (by cold drawing, solid-state extrusion, or rolling) or from the melt in an extensional-flow setup in which the material is allowed to crystallize.[2] The high-tensile properties of oriented polymers are caused by the intrinsic anisotropy of polymers and are connected with their chainlike structure. Along the backbone of the oriented chains the strength is determined by covalent interactions that are much more energetic than those of the van der Waals type that predominate in unoriented samples.

It is now well-established that the conformation of a polymer molecule can change significantly in an elongational flow field.[3,4] In this type of flow the dominant component of the velocity is parallel to the flow direction. Under appropriate conditions, chains can achieve nearly full extension near the stagnation point, where the strain rate is the highest. Theoretically, the influence of this type of flow on an isolated polymeric coil was studied by De Gennes,[5] who used in his description an earlier theory of Peterlin,[6,7] and predicted a sharp coil−stretch transition at a critical strain rate. Although theories describing the coil−stretch transition focus on polymer solutions, the same principles apply, mutatis mutandis, to polymeric melts.

The coil−stretch transition is important in the context of flow-induced crystallization, for there is experimental evidence[1] that polymeric chains stretched in elongational flow solidify into a fiber core, also known as a "shish", which subsequently acts as a nucleation center that enhances the nucleation of crystallites of chains on it.[1,9] The crystalline lamellar structures (the so-called "kebabs"), in which the chains are *not* completely stretched, have a tendency to attach to this central core upon solidification. This has been observed in many experiments[1] but also in recent computer simulation studies.[8,9]

The competition between the influence of an external field that tends to increase order, and the random-walk nature of the polymers in the melt, which promotes disorder, should be an essential ingredient in any sensible theoretical description of flow-induced solidification. Although an inherently nonequilibrium problem, a kinetic theory that does not account for this through the input of a free energy landscape that explicitly deals with the chainlike nature of polymers is bound to fail. In fact, even in the absence of flow a sensible description of the crystallization of polymers requires a self-consistent coupling between the configurational statistics of the chains and the thermodynamics of the crystallization transition.[10]

In this context it may be useful to refer to the idea of Flory[11] that chain stiffness in combination with packing effects must be at the root of the solidification of polymers. Despite being largely ignored by the polymer crystallization community, this has been confirmed by means of computer simulations.[12] Indeed, repulsive interactions are sufficient to induce crystallization in model polymeric systems—even the familiar lamellar structure is reproduced.[8,12]

Here, we consider the role of an external field mimicking elongational flow in the entropy-driven solidification of model polymers. We shall not be focusing on strong flows in which the chains strongly deform but instead deal with how a weak flow affects the packing of the polymer segments in the melt. These packing effects ultimately promote crystallization. As we shall see, even at this level of approach a strong impact on the stability of the crystal phase is observed. Depending on the flow type and the crystal symmetry, the crystal phase may be either stabilized or destabilized, or one crystal symmetry be favored over another.

We note that the coupling of flow fields to phase transitions has attracted a considerable attention from both theorists and experimentalists, in particular in the field of the isotropic-to-nematic phase transition of stiff polymers and of other rodlike particles.[13−18] This transition is also entropy dominated. From these studies we infer that an external flow field (shear or elongational flow) promotes liquid-crystalline ordering because the external field increases the degree of order in the

† Present address: Laboratory of Polymer Chemistry, University of Groningen, Nijenborgh 4, 9747 AG Groningen, The Netherlands. E-mail: N.Sushko@chem.rug.nl.

10.1021/ma034864r CCC: $27.50
Published on Web 12/13/2003

system. Another point of interest in the context of our studies is that even a weak flow has a noticeable effect on the demixing of polymeric systems. On the basis of a theoretical thermodynamic analysis, Bhattacharjee et al.[19] found that in sufficiently weak two-dimensional elongational flow, i.e., far from coil−stretch transition, there are flow-induced shifts of the so-called θ-point and of the coexistence curve for polymers in solution.

In this work we present a mean-field analysis of the role of a weak orienting field on the crystallization of a model polymeric melt. We assume that the system is in a state of local equilibrium, and that the flow is steady and of a potential type, to be able to apply a Kramers potential description[20] of the flow. Our aim is not to reproduce the shish-kebab or any other type of supramolecular structure that is often found after a crystallization in flow. Instead, we aim to shed light on the possible impact that a flow field may have on the coupling of chain configurations, packing effects, and the stability of the crystal phase. To this end we make use of an amalgamation of the Green function description of a polymer chain in a self-consistent field and classical density functional theory. The Kramers potential we use mimics two types of flow, elongational flow and longitudinal shear. We show that a weak elongational flow field stabilizes the polymeric crystal, while longitudinal shear destabilizes the crystalline state.

The remainder of this paper is organized as follows. In section 2 we first briefly describe the model polymers considered and the theoretical formalism used to study the influence of an external orientational field on the crystallization. The application of the calculation method to the face-centered cubic (fcc) and hexagonal close-packed (hcp) crystal geometry is explained in section 3. The results of our numerical calculations are given in section 4, and our conclusions are presented in section 5.

2. Polymeric Density Functional Theory

We apply a recently proposed[21] polymeric density functional theory (DFT). The model polymers consist of N beads that interact through a hard-core repulsive potential and that are connected by freely hinged phantom bonds with an adjustable bond stiffness. The single-chain partition function, or Green function,[22] of a chain with its ends fixed at the positions $\mathbf{r}$ and $\mathbf{r}'$ can be written as

$$Z_N(\mathbf{r}',\mathbf{r};1,N) = \int \left(\int_{j=1}^{N} \mathrm{d}\mathbf{r}_j\right) \delta(\mathbf{r}_1 - \mathbf{r}')\, \delta(\mathbf{r}_N - \mathbf{r}) \times \left(\int_{j=2}^{N} g(\mathbf{r}_j,\mathbf{r}_{j-1}) \exp[-\beta U_{\mathrm{scf}}(\mathbf{r}_j) - \beta U_{\mathrm{ext}}(\mathbf{r}_j,\mathbf{r}_{j-1})]\right) \quad (1)$$

with $U_{\mathrm{scf}}(\mathbf{r}_j)$ the self-consistent molecular field that a monomer labeled $j = 1, ..., N$ on an arbitrary test chain experiences due to the presence of other polymeric chains and $U_{\mathrm{ext}}(\mathbf{r}_j,\mathbf{r}_{j-1})$ an external orienting field that couples to pairs of neighboring monomers j and $j - 1$. Note that the self-consistent molecular field is a function of a single positional coordinate because we study freely hinged model chains that interact via pairs of site−site interactions only. As usual, $\beta \equiv 1/k_{\mathrm{B}}T$, where T denotes the absolute temperature and k_{B} Boltzmann's constant.

In eq 1, the "kernel" $g(\mathbf{r},\mathbf{r}')$ represents the bonded interactions between consecutive beads on a chain through the normalized a priori probability that a bond that starts at position $\mathbf{r}'$ ends at position $\mathbf{r}$. It is a model-dependent quantity. For our model polymer we define this probability, such that it interpolates between the standard Gaussian and Kuhn models,[21]

$$g(\mathbf{r} - \mathbf{r}') = \frac{\sqrt{6}}{8\pi^{3/2}\xi|\mathbf{r} - \mathbf{r}'|\, l}\left(\exp\left[-\frac{3(|\mathbf{r} - \mathbf{r}'| - l)^2}{2\xi^2}\right] - \exp\left[-\frac{3(|\mathbf{r} - \mathbf{r}'| + l)^2}{2\xi^2}\right]\right) \quad (2)$$

where l is a mean length of the bonds and ξ is a root-mean-square deviation from this length. The effective Kuhn length l_{K} of the model may be expressed in terms of l and ξ, as $l_{\mathrm{K}} = \sqrt{l^2+\xi^2}$.[21] We distinguish two regimes: one where our model behaves like a freely hinged chain model for $\xi \ll l$ with fixed bond length $l_{\mathrm{K}} = l$ and one where it becomes equivalent to the standard Gaussian-chain model with a root-mean-square bond extension $l_{\mathrm{K}} = \xi$, corresponding to the limit $\xi \gg l$. In this paper we present results only for the Gaussian-chain limit, although we have performed calculations in the other (freely hinged, Kuhn) limit as well. However, the somewhat erratic character of the data obtained for the latter limit proved hard to interpret and in addition required excessive computational effort to remove numerical inaccuracies. (See also below.)

Equation 1 can be rewritten in terms of a recursive equation

$$Z(\mathbf{r}', \mathbf{r}; 1, N+1) = \exp[-\beta U_{\mathrm{scf}}(\mathbf{r})] \int \mathrm{d}\mathbf{r}''\, g(\mathbf{r}', \mathbf{r}'') \times \exp[-\beta U_{\mathrm{ext}}(\mathbf{r}', \mathbf{r}'')] Z(\mathbf{r}'', \mathbf{r}; 1, N) \quad (3)$$

subject to the boundary condition $\lim_{N\to 1} Z(\mathbf{r}',\mathbf{r};1, N) = \exp[-\beta U_{\mathrm{scf}}(\mathbf{r}))]\delta(\mathbf{r}' - \mathbf{r})$. The solution to this recursive equation eq 3 is a bilinear sum of products of the left and right eigenfunctions of the integral operation, weighed by the corresponding eigenvalue to the power N.[23−25]

The total partition function of the system of M polymeric chains is $\mathcal{Z} = (1/M!)Z_N^M$, where $Z_N \equiv \int \mathrm{d}\mathbf{r} \int \mathrm{d}\mathbf{r}'\, Z(\mathbf{r}',\mathbf{r}; 1, N)$ is the single-chain partition function. The Helmholtz free energy F of the system can be easily obtained from the thermodynamic relation $\beta F = -\ln \mathcal{Z}$. The molecular field $U_{\mathrm{scf}}(\mathbf{r})$ we treat as an external field, and we use the procedure pioneered by Lifshitz[26] in order to determine this field. To this end, the configurational part F_{conf} of the free energy is calculated by a subtraction of the self-consistent-field energy $\int \mathrm{d}\mathbf{r}\, U_{\mathrm{scf}}(\mathbf{r})\, \rho(\mathbf{r})$ from the free energy F of the system. Here, $\rho(\mathbf{r})$ notes the number density of segments given by

$$\rho(\mathbf{r}) \equiv M Z_N^{-1} \sum_{s=1}^{N} \int \mathrm{d}\mathbf{r}' \int \mathrm{d}\mathbf{r}''\, Z(\mathbf{r}', \mathbf{r}; 1, s)\, Z(\mathbf{r}, \mathbf{r}''; s, N) \quad (4)$$

Within the self-consistent-field method, the actual free energy $\mathcal{F}$ is a sum of the configurational free energy and the excess free energy, F_{exc}, which accounts for the interaction between the segments

$$\mathcal{F} = F_{\mathrm{conf}} + F_{\mathrm{exc}} \quad (5)$$

The density dependence of the configurational free energy can be made explicit. We apply a ground-state approximation and use only the largest eigenvalue. For use in a DFT of the crystal phase, it turns out useful to expand the density $\rho(\mathbf{r}) = \rho_{\mathrm{L}} + \Delta\rho(\mathbf{r})$ around that of the

liquid state, ρ_L, and neglect the terms of higher than second order in perturbation $\Delta\rho$. Applying the methodology presented in ref 21, we find for difference between the configurational free energy of the solid and that of the melt

$$\beta\Delta F_{conf} = \int d\mathbf{r}\ \rho(\mathbf{r}) \ln \rho(\mathbf{r}) - \int d\mathbf{r}\ \rho_L \ln \rho_L - \frac{1}{\rho_L}\int d\mathbf{r} \int d\mathbf{r}'\ \Delta\rho(\mathbf{r}) e^{-\beta U_{ext}(\mathbf{r},\mathbf{r}')} g(\mathbf{r}, \mathbf{r}')\Delta\rho(\mathbf{r}) + O(\Delta\rho^3) \quad (6)$$

where the first two terms are the free energies of the ideal solid and melt and the third term enters due to the connectivity of the polymers. A consequence of the ground-state approximation is that eq 6 only describes (positional) ordering on short wavelengths, although the coupling to the external field described next does not preclude long-range configurational effects.

For the Kramers potential we write[15,20]

$$\beta U_{ext} = -\frac{3}{2} u \cos^2 \epsilon \quad (7)$$

where u is a dimensionless field strength that we later on connect with the actual elongational flow rate and ϵ the angle between the direction of a bond of a test chain and the direction of the field $\mathbf{n}$, $\cos\epsilon \equiv \mathbf{n}\cdot(\mathbf{r} - \mathbf{r}')/|\mathbf{r} - \mathbf{r}'|$. Hence, the potential couples not to single monomers but to pairs of monomers at the positions $\mathbf{r}$ and $\mathbf{r}'$. Positive and negative values of u correspond to different flow geometries. The case where u is positive corresponds to inhomogeneous vortex-free longitudinal shear. When u is negative, the quadrupole potential models a hydrodynamic flow acting on the polymers confined within an unaxially compressed sample.

We switch on the Kramers potential not only in the description of the melt but also in that of the crystal phase. The reason this is justified is that the chains are orientationally preordered in the flow before crystallizing. This implies that it is necessary to allow for a redistribution of the bonds on the crystal lattice through the influence of the Kramers potential. Note that this does not mean that the angular distribution of the bonds in melt and crystal phases are equal. As we shall see this below, circumstance provides a possible explanation for our finding that one type of the flow ($u < 0$) stabilizes the crystal, when another one ($u > 0$) destabilizes the crystal phase. We assume that the crystal lattice itself is not deformed by the flow on the level of a single unit cell.

For computational convenience we do not employ the Helmholtz free energy, but the grand potential.[21] The grand-potential difference $\Delta\Omega[\rho(\mathbf{r})]$ between the crystal and a liquid reference state is[27]

$$\beta\frac{\Delta\Omega}{\rho_L V} \equiv \Delta\omega = \frac{1}{\rho_L V}\int d\mathbf{r}\ \rho(\mathbf{r}) \ln \rho(\mathbf{r})/\rho_L - \frac{1}{{\rho_L}^2 V}\int d\mathbf{r}'\ g_F(|\mathbf{r} - \mathbf{r}'|)[\rho(\mathbf{r}) - \rho_S][\rho(\mathbf{r}') - \rho_S] - \frac{1}{\rho_L V}\sum_{p=2}^{\infty}\frac{1}{p!}\int \cdots \int C^{(p)}(\mathbf{r}_1,...,\mathbf{r}_p)\prod_{i=1}^{p} d\mathbf{r}_i\,(\rho(\mathbf{r}_i) - \rho_L) - \beta(\mu_S - \mu_L)\frac{1}{\rho_L V}\int d\mathbf{r}\ \rho(\mathbf{r}) - \frac{1}{\rho_L V}\int d\mathbf{r}\ (\rho(\mathbf{r}) - \rho_L) \quad (8)$$

where we take the configurational term to first order in the density difference between the two phase and the excess term to arbitrary order in this difference (although below we truncate this term at the third order). In eq 8, V is the volume of the system, μ_S is the chemical potential of the solid, μ_L is that of the liquid reference phase, and ρ_S and ρ_L are the segment densities of respectively the solid and liquid state; $g_F(|\mathbf{r} - \mathbf{r}'|)$ is a field-modified kernel defined below.

As we show in previous work,[21,27] the p-particle direct correlation function of the liquid reference state $C^{(p)}(\mathbf{r}_1,...,\mathbf{r}_p) = -\beta\delta^{(p)}F_{exc}/\prod_{i=1}^{p}\delta\rho(\mathbf{r}_i)$ can be calculated from a similar free energy as given in eq 8, producing an integral equation equivalent to that of the polymeric reference interaction site model (the so-called PRISM equation).[28] The chain-connectivity effect is described directly through the second term in the right-hand side of eq 8 and indirectly via the direct correlation functions in the third term.

The PRISM equation, which connects the total correlation function of two segments on different chains, $h(\mathbf{r},\mathbf{r}')$, and the associated two-particle direct correlation function, $C^{(2)}(\mathbf{r},\mathbf{r}')$, reads in Fourier space

$$\hat{h}(\mathbf{q}) = \hat{\omega}(\mathbf{q})\,\hat{C}^{(2)}(\mathbf{q}) + \rho_L\hat{\omega}(\mathbf{q})\,\hat{C}^{(2)}(\mathbf{q})\,\hat{h}(\mathbf{q}) \quad (9)$$

where the hats indicate Fourier transformed quantities, $\mathbf{q}$ is the wave vector, and ρ_L is the average melt density. The intramolecular correlations between segments on a single chain are described by the form factor $\hat{\omega}$

$$\hat{\omega}(q) = \frac{1 - \hat{g}_F{}^2 - \frac{2}{N}\hat{g}_F + \frac{2}{N}\hat{g}_F{}^{N+1}}{(1 - \hat{g}_F)^2} \quad (10)$$

where $\hat{g}_F$ is the Fourier transform of the bond probability in the presence of the orienting field. To calculate this quantity, we assumed this field to be weak, so that $g_F(\mathbf{r},\mathbf{r}') \equiv \exp[-\beta U_{ext}(\mathbf{r}, \mathbf{r}')]g(\mathbf{r},\mathbf{r}') \simeq g(\mathbf{r},\mathbf{r}')(1 - \beta U_{ext}(\mathbf{r}, \mathbf{r}'))$ in the limit $\xi \gg l$, i.e., for the standard Gaussian model. We find

$$\hat{g}_F(q) = \exp\left[-\frac{q^2 {l_K}^2}{6}\right]\left\{1 + \frac{1}{2}u(1 + 2P_2(\cos\gamma) + 18q^{-2}{l_K}^{-2}P_2(\cos\gamma))\right\} - 9uq^{-3}{l_K}^{-3}\sqrt{6\pi}P_2(\cos\gamma)\frac{\mathrm{erf}(ql_K)}{2\sqrt{6}} \quad (11)$$

where q is the length of the vector in Fourier space and γ the angle between the direction of field $\mathbf{n}$ and the vector $\mathbf{q}$ in Fourier space. The details of calculation of the kernel $g_F(\mathbf{r},\mathbf{r}')$ in the presence of an external field can be found in the Appendix. Equation 9 is valid at nonzero external field, since the chains remain freely hinged even when under an external field and nonideal bond-order correlations cannot build up on account of the isotropic site−external interactions presumed in this work.

We use the classical Percus−Yevick (PY) closure to solve eq 9,[29] mimicking a hard-core interaction between the polymeric beads. As for the terms of higher order than second order of the direct correlation functions,

below we extract the zero-$\mathbf{q}$ $\hat{C}^{(3)}$ from $\hat{C}^{(2)}$ and ignore fourth- and higher-order terms.[21,30] See also eq 15.

3. Solidification into the Close-Packed-Crystal Geometry

Ideally, one calculates the equilibrium density profiles in the crystal phase by a functional free-energy minimization. It is computationally more convenient, however, to use an Ansatz for $\rho(\mathbf{r})$ and optimize this Ansatz. For the density distribution $\rho(\mathbf{r})$ in the crystal phase we use the Gaussian profile

$$\rho(\mathbf{r}) = (\pi\epsilon^2)^{-3/2} \sum_{\{\mathbf{R}_n\}} \exp[-(\mathbf{R}_n - \mathbf{r})^2/\epsilon^2] \qquad (12)$$

where $\{\mathbf{R}_n\}$ is the set of all real-space crystal-lattice vectors and ϵ is a variational parameter that measures of the width of the Gaussian density distribution around each point of the crystal lattice. It turns out to be useful to write eq 8 in terms of a Fourier representation of the density distribution eq 12,

$$\rho(\mathbf{r}) = \rho_L[1 + \eta + \sum_{\{\mathbf{q}\}} \zeta(\mathbf{q}) \exp(i\mathbf{q}\cdot\mathbf{r})] \qquad (13)$$

with $\{\mathbf{q}\}$ the set of the reciprocal-lattice vectors of the crystal lattice under consideration, $\eta = (\rho_S - \rho_L)/\rho_L$ the dimensionless density jump across the crystallization transition, and

$$\zeta(\mathbf{q}) = (1 + \eta) \exp[-\mathbf{q}^2\epsilon^2/4] \qquad (14)$$

We insert eq 13 into eq 8, truncate the sum containing the direct correlation functions after the third term, and obtain the following expression for the grand potential:

$$\Delta\omega = 1 - (1 + \eta)\left(^5/_2 + \ln\rho_L + {}^3/_2 \ln \pi\epsilon^2 - \frac{1}{k_B T}(\mu_S - \mu_L)\right) - \sum_{\{\mathbf{q}\}} \hat{g}_F(\mathbf{q})\, \zeta^2(\mathbf{q}) - \frac{1}{2}\eta^2\rho_L \hat{C}_L^{(2)}(0) - \frac{1}{2}\rho_L \sum_{\{\mathbf{q}\}} \zeta^2(\mathbf{q})\, \hat{C}_L^{(2)}(|\mathbf{q}|,\gamma) - \frac{1}{6}\eta^3\rho_L{}^2 \hat{C}_L^{(3)}(0,0) \qquad (15)$$

In our density functional we include only the zero-q part of the three-body direct correlation function[30]

$$\hat{C}_{L(3)}(0, 0) = \lim_{q\to 0} \hat{C}_L^{(3)}(q,0) = \lim_{q\to 0} \frac{\partial \hat{C}_L^{(2)}(q)}{\partial\rho}|_{\rho=\rho_L} \qquad (16)$$

because local contributions are usually deemed to be unimportant.[30,31] To obtain the optimal density profiles in the crystal phase, we minimize eq 15 with respect to the liquid density ρ_L, the parameter η, and also the width of the density profile ϵ. It should be stressed that as a result of the ground-state approximation long-range orientational bond order can only develop in our model through the coupling to the external orienting field. In the absence of such a field, the chains behave like random walkers on the crystal lattice.[21]

The crystal types we consider are of the face-centered cubic (fcc) and of the hexagonal close-packed (hcp) type. The reciprocal to the fcc lattice is the body-centered cubic (bcc) lattice. The set of the reciprocal vectors $\{\mathbf{q}\}$ that enters the grand potential eq 15 can be calculated from the following expression

$$\mathbf{G} = \frac{2\pi}{a}[(h - k + l)\mathbf{i} + (h + k - l)\mathbf{j} + (-h + k + l)\mathbf{k}] \qquad (17)$$

with h, k, and l integers, a the nearest-neighbor separation, and $\mathbf{i}$, $\mathbf{j}$, and $\mathbf{k}$ the basis vectors in the Cartesian system of coordinates. We arbitrarily choose the following bcc axis as the main axis in order to describe the orientation of the crystal in space

$$\mathbf{G}^0 = \frac{2\pi}{a}[\mathbf{i} + \mathbf{j} - \mathbf{k}] \qquad (18)$$

The geometry of the model in the case of the fcc lattice is shown in Figure 1. In our calculations enters the angle γ between the direction of an external field $\mathbf{n}$ and the vector $\mathbf{q}$ through the bond probability eq 11. The angle between the main axis $\mathbf{G}^0$ of the reciprocal lattice and the direction of an external field $\mathbf{n}$ can be expressed in Cartesian coordinates via usual polar angles θ and ϕ. For the fcc lattice, these angles are connected to the angle γ by a simple trigonometric relation

$$\cos\gamma = \cos\theta \frac{3h - k - l}{\sqrt{9(h^2 + k^2 + l^2) - 6(hk + hl + kl)}} + \sin\theta \sqrt{1 - \frac{(3h - k - l)^2}{9(h^2 + k^2 + l^2) - 6(hk + hl + kl)}} \cos\phi \qquad (19)$$

For the case of the hcp lattice, the set of the reciprocal vectors can be calculated from the expression

$$\mathbf{G} = \frac{2\pi}{a}\left[h\,\mathbf{i} + \frac{1}{\sqrt{3}}(h + 2k)\mathbf{j} + \frac{a}{c}l\,\mathbf{k}\right] \qquad (20)$$

where $c/2$ is the separation of neighboring hexagonal planes. We choose the following axis as a main one

$$\mathbf{G}^0 = \frac{2\pi}{a}\left[\mathbf{i} + \frac{1}{\sqrt{3}}\mathbf{j}\right] \qquad (21)$$

and the angle γ can be found from the relation

$$\cos\gamma = \cos\theta \frac{\frac{1}{\sqrt{3}}(2h + k)}{\frac{4}{3}(h^2 + hk + k^2) + (al/c)^2} + \sin\theta\cos\phi \sqrt{1 - \frac{(2h + k)^2}{4(h^2 + hk + k^2) + \frac{1}{3}(al/c)^2}} \qquad (22)$$

We minimize eq 15, using the standard quasi-Newton algorithm from the NAG library (Mark 18, E04JYF), at the coexistence between the liquid and solid phases, when the pressures and chemical potentials in both phases are equal.

The number of reciprocal lattice vectors $\{\mathbf{q}\}$ needed to accurately describe the fcc and/or hcp crystal phase we determine empirically. (In the absence of an external field, 5832 reciprocal lattice vectors are needed to get accurate results.[21]) In the presence of the field the direct correlation function has to be evaluated for each value of the angle γ, which is different for every reciprocal lattice vector, to reach the desired precision. We perform calculations of the direct correlation function for a few

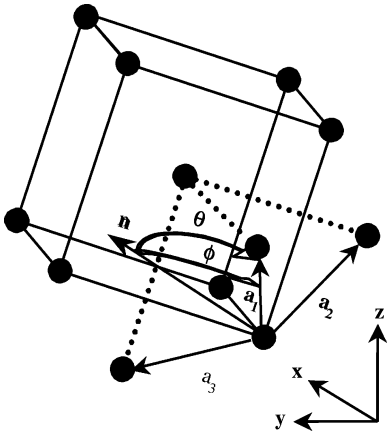

Figure 1. The bcc lattice is reciprocal to the fcc structure. Shown are also the geometrical parameters of the model under consideration. The vector **n** shows the direction of an external field, the vectors $\mathbf{a}_1$, $\mathbf{a}_2$, $\mathbf{a}_3$ denote the primitive translation vectors of the bcc lattice, and the angle between the arbitrary chosen main axis $\mathbf{G}^0 \equiv \mathbf{a}_1$ and direction of an external field **n** can be expressed in Cartesian coordinates via the usual polar angles θ and ϕ.

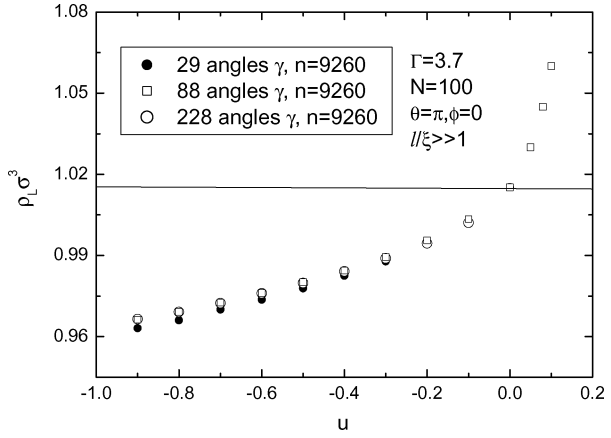

Figure 2. Freezing density of the polymeric liquid in the Gaussian-chain limit $\xi/l \gg 1$ if the solid phase has a fcc lattice, as a function of the strength of external field u. Orientation angles $\theta = \pi$ and $\varphi = 0$ of the lattice. See Figure 1. Chain parameters $\Gamma = 3.7$ and $N = 100$.

thousand reciprocal lattice vectors. Fortunately, the direct correlation function is only a sensitive function of the angle γ, and therefore of the field, in the small-**q** regime. Thus, the direct correlation function in the presence of the field needs to be evaluated only for the first few shells of the reciprocal lattice. For the remaining shells the field-free results for the direct correlation function are sufficiently accurate. That this is so is shown in Figure 2 for the fcc lattice, where we plot the freezing density of the liquid for the case when the angle dependencies of the first five shells (29 reciprocal lattice vectors), the first 10 shells (88 reciprocal lattice vectors), and the first 20 shells (228 vectors) are included. The total number of reciprocal lattice vectors we use is 9260. It seems sufficient to take into account the values of the angle γ only for the first 88 reciprocal lattice vectors.

In the next section we discuss the results of our calculations.

4. Results and Discussion

Before discussing the results, it seems useful to clarify the physical meaning of the parameter u, which in our calculation denotes the strength of an external field

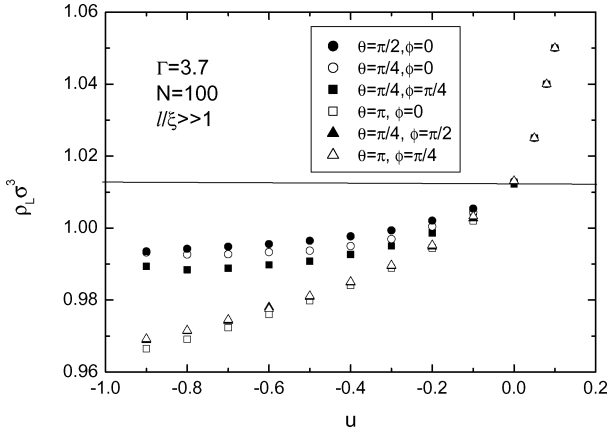

Figure 3. Freezing density of the polymeric liquid in the Gaussian-chain limit ($\xi/l \gg 1$) as a function of the strength of external field u, for different values of the orientation angles θ and φ of the fcc lattice, at fixed $\Gamma = 3.7$ and $N = 100$.

acting on a single bond. To connect this parameter with a flow rate, we presume that the chains are not very long so that they obey Rouse dynamics. The relaxation time and radius of gyration can be determined analytically for a test chain in a weak Kramers potential flow from the Smoluchowski equation for the configurational distribution function.[32] Comparing the radius of gyration of our model and that obtained by Frisch et al.[32] for the Rouse model, we conclude that the parameter u must be equal to $2\tau_0^2 s^2$, where s is the flow rate and τ_0 the characteristic relaxation time of the chain, often called the Kramers relaxation time. This relaxation time τ_0 is proportional to the square of the number of monomeric units per chain and corresponds, apart from an uninteresting numerical multiplicative constant, to the well-known Rouse time of the chain.[32]

Apart from the field strength (flow rate) u and the degree of polymerization N, the only control parameter that we have is a quantity that we call the fusion parameter $\Gamma \equiv l_K/\sigma$, where l_K is the effective Kuhn length of the chains and where σ indicates the range of the hard-core interactions. We calculated the dependence of the freezing density on the parameter u for the standard Gaussian model, $\xi/l \gg 1$, for different orientations of the crystal lattice relative to the main axis of the flow field at fixed degree of polymerization $N = 100$ and fusion parameter $\Gamma = 3.7$ and show the results in Figure 3. (The crystal type is fcc.) It shows that the polymeric melt crystallizes more easily under the influence of an external ordering field than in the absence of this field at all values of the polar angles of orientation θ and ϕ between the direction of the external field and the main axis of the lattice, but only when the parameter u is negative. If it is positive, the freezing density goes up.

A possible cause for this is the following. For positive u, the orientation of the induced anisotropy of polymeric melt is parallel to the direction of the field. This makes it more difficult for a polymeric bead to occupy a free lattice site in the presence than in the absence of this field. When u is negative, the anisotropy is induced in the easy plane, with a symmetric distribution of the polymeric segments relative to the lattice axes. Hence, in the present crystal geometry it is easier to crystallize in fcc lattice when u is a negative.

Figure 4 presents a structural explanation of the stability of the crystal phase for different values of u

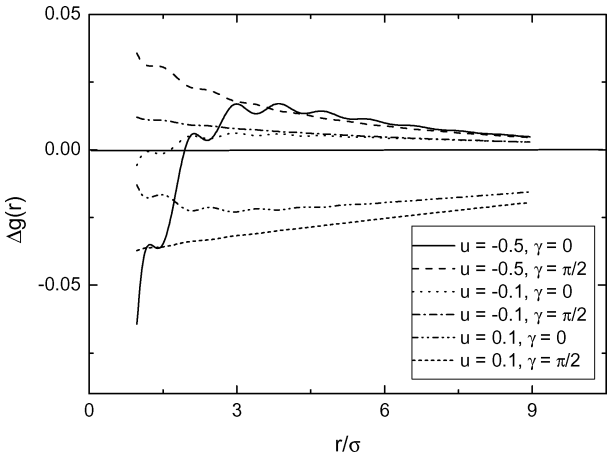

Figure 4. Difference $\Delta g(r)$ between the pair-correlation function of the polymeric melt in the presence of an external field and the pair-correlation function of the melt in the absence of this field as a function of a dimensionless distance r/σ, for different values of the strength of an external field u and the angle γ (see the main text). The density $\rho_L = 0.96\sigma^3$ and the chain parameters are fixed at $\Gamma = 3.7$ and $N = 100$.

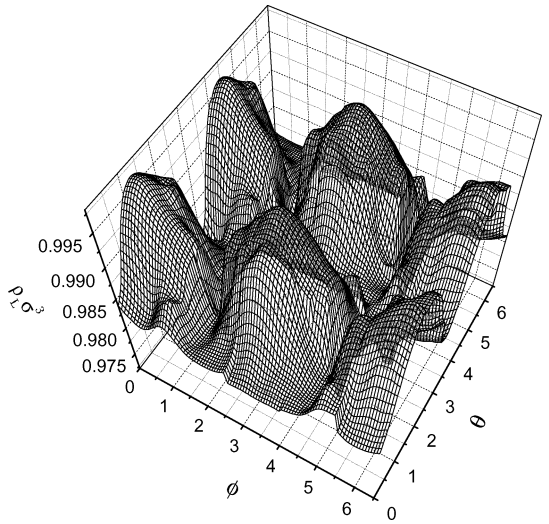

Figure 5. Freezing density of the polymeric liquid as a function of the lattice-orientation angles θ and φ. The figure shows results for the fcc lattice for the parameter values $\Gamma = 3.7$, $u = -0.5$, and degree of polymerization $N = 100$ in the Gaussian chain limit $\xi/l \gg 1$.

and for different orientations of the lattice with respect to the field. The difference $\Delta g(r)$ between the pair-correlation function of the polymeric melt in the presence of an external field and the pair-correlation function of the melt in the absence of this field is (largely) positive when $u < 0$ and negative when $u > 0$. In other words, the orienting field induces stronger positional correlations in the melt if $u > 0$, diminishing the structural difference between the melt and the crystal phase, thereby stabilizing the latter. When $u > 0$, this difference is negative for all angles γ: the field destroys local positional order in the melt with the opposite effect of destabilizing the crystal phase.

The next, three-dimensional plot of Figure 5 shows the orientation dependence of the freezing density at fixed value of the parameter $u = -0.5$ and fusion parameter $\Gamma = 3.7$, again for $N = 100$. The dependence on the angles θ and φ of the lattice orientation has a nontrivial character. There is an obvious periodicity, albeit that this effect is small; the difference between

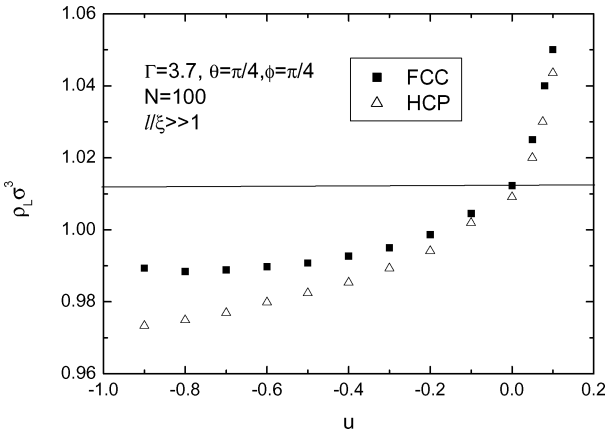

Figure 6. Comparison of the freezing density of the polymeric liquid in the Gaussian chain limit $\xi/l \gg 1$ for the fcc and hcp lattices as a function of the strength of external field for the angles $\theta = \pi/4$ and $\varphi = \pi/4$, at fixed $\Gamma = 3.7$ and $N = 100$. The hcp lattice crystallizes at lower density if under an external field.

the maximal and minimal values for the freezing densities found is just a few percent. Global minima in the freezing density are found close to the angles $\theta = \pi k$ and $\phi = \pi k/2$, with k an integer. Figure 5 demonstrates the importance of geometrical effects in the determination of the freezing density of the polymeric melt.

Now we compare the freezing of the fcc and hcp structures under an external field for the arbitrarily chosen angles $\theta = \pi/4$ and $\phi = \pi/4$, again in the Gaussian chain limit $\xi/l \gg 1$ (see Figure 6). Only the ideal hcp lattice was considered, i.e., $c/a = (8/3)^{1/2}$. In the absence of an external field the fcc and hcp structures of hard Gaussian chains are equally probable within our DFT and within the accuracy of the numerics that we estimate to be about 0.5%. (For a discussion on the relative stability of the fcc and hcp lattice types as a function of the bond stiffness, see ref 27.) When the external field is switched on, both lattices crystallize at a lower density than in the absence of the field, but the hcp structure crystallizes at a lower density and should therefore be more stable. Thus, not only the mean length and the stretching stiffness of the bonds can determine the lattice type, as we concluded in earlier work,[27] but also the presence of an external field. Note that the crystal type may remain metastable if the field is turned off and that the relative stability of the hcp and fcc crystals may depend on their orientation in the external field.

In Figure 7 we show the dependence on the fusion parameter Γ of the fcc and hcp freezing densities in the presence of an external field, for $u = -0.5$ and $u = 0$. The orientation of the crystal was fixed at the arbitrary angles $\theta = \pi/4$ and $\phi = \pi/4$. The difference in freezing densities is significant only in the small-Γ regime. In this regime the system crystallizes more easily under the influence of an external field. In the large-Γ regime the behavior of the polymeric system is monomer-like. In that case the external orientational field cannot influence the stability of the crystal phase.

Finally, in Figure 8 we examine how the degree of polymerization N affects the crystallization density of the model polymers in an external orientational field, at a fixed fusion parameter of $\Gamma = 3.7$ and at fixed angles $\theta = \pi/4$ and $\phi = \pi/4$ (again chosen arbitrarily). From Figure 8 it can be seen that in the absence of an external

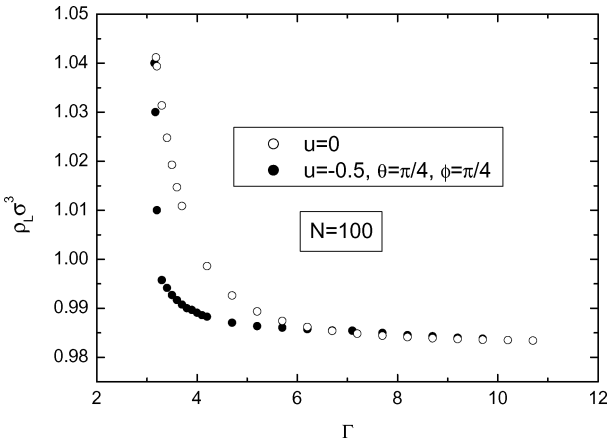

Figure 7. Freezing density of the polymeric liquid in the Gaussian chain limit $\xi/l \gg 1$ as a function of the fusion parameter Γ for the fcc lattice. Compared are values in the absence of the field and when $u = -0.5$ and angles $\theta = \pi/4$, $\varphi = \pi/4$.

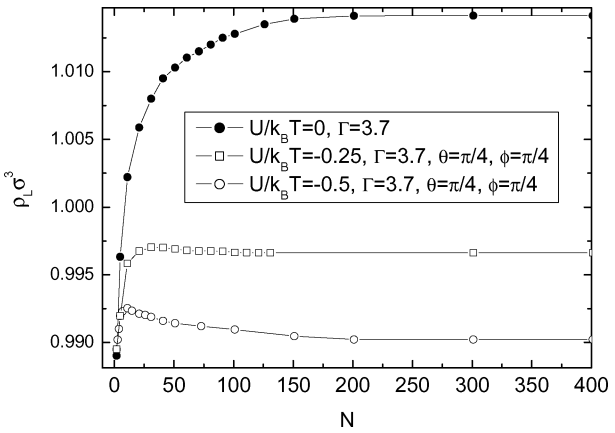

Figure 8. Freezing density of the polymeric liquid in the Gaussian-chain limit $\xi/l \gg 1$ for the fcc lattice as a function of degree of polymerization N for different values of u at fixed $\Gamma = 3.7$ and angles $\theta = \pi/4$, $\varphi = \pi/4$.

field an increase in the degree of polymerization destabilizes the crystal.[21] It turns out that the dependence of the crystallization density on N in the presence of the external field becomes nonmonotonic. For long chains ($N \geq 200$) the freezing density saturates, while for relatively short chains ($N \leq 10$) there is no significant influence of an orienting field. We have no explanation for this.

5. Conclusions

We find that our model polymers crystallize more easily in an external field of the quadrupole type than in absence of that field, but only if it is a so-called disorienting field, corresponding to a longitudinal shear setup. Geometric effects, such as the direction of the field with respect to the orientation of the lattice, play an important role in the stability of the crystal phase. We find that the competition between configurational entropy of the chain and the strength of a field that couples to individual bonds leads to a nontrivial flow dependency of the stability of the model polymeric solid. Finally, it appears that the presence of an external field can stabilize one lattice type over another.

Appendix: The Fourier Transform of the Bond Probability in the Presence of an External Orientational Field

In this appendix we calculate the Fourier transform of the bond probability in the presence of a quadrupole field. In the presence of a weak enough external field, it can be expressed as

$$g_F = g(\mathbf{r}, \mathbf{r}')e^{-\beta U_{ext}(\mathbf{r},\mathbf{r}')} \simeq g(\mathbf{r}, \mathbf{r}')(1 - \beta U_{ext}(\mathbf{r}, \mathbf{r}')) \quad (23)$$

For U_{ext} we use the Kramers potential, eq 7. We presume that the external field does not change the length of a single polymeric bond and only changes the orientation of this bond. This assumption seems to be quite reasonable for weak external fields, i.e., far from the coil−stretch transition.[33]

We apply the following geometry. The angle between the director of a field $\mathbf{n}$ and the vector $\mathbf{q}$ in Fourier space we denote as γ, the angle between vector $\mathbf{r} - \mathbf{r}'$ and $\mathbf{n}$ we mark as ϵ, and, finally, the angle between $\mathbf{r} - \mathbf{r}'$ and $\mathbf{q}$ we denote as α. The following trigonometric relationship in spherical coordinates (r,α,ψ) holds

$$\cos\epsilon = \cos\gamma\cos\alpha + \sin\gamma\sin\alpha\cos\psi \quad (24)$$

We perform the Fourier transformation of the full function of the length ξ in eq 2,

$$\hat{g}_F = \int_0^{2\pi} d\psi \int_{-\pi}^{\pi} \sin\alpha\, d\alpha \int_0^{\infty} r^2\, dr\, g(r)\Big(1 + \frac{3}{2}u(\cos^2\gamma\cos^2\alpha + \sin^2\gamma\sin^2\alpha\cos^2\psi + \sin 2\gamma\cos\alpha\sin\alpha\cos\psi)\Big)\exp[iqr\cos\alpha] \quad (25)$$

to obtain

$$\hat{g}_F(q) = \exp[-q^2\xi^2/6]\Big\{\sin(ql) + {}^3/_4 uq^{-1}l^{-1}\sin(ql_K)(1 + \cos 2\gamma) + \frac{9}{4}uq^{-3}l^{-1}\xi^{-2}\sin(ql_K)(1 + 3\cos 2\gamma)\Big\}q^{-1}l^{-1} - \frac{9}{16}u\sqrt{6\pi}q^{-3}\xi^{-3}\exp(-{}^3/_2 l_K{}^2/\xi^2) \times \Big\{\mathrm{erf}\,\frac{\xi^2 q - 3il}{\sqrt{6}\xi} + \mathrm{erf}\,\frac{\xi^2 q + 3il}{\sqrt{6}\xi}\Big\}(1 + 3\cos 2\gamma) \quad (26)$$

where erf denotes the standard error function. Note that the sum of error functions in the last term is always real. In the absence of an external field, the expression above simplifies to the familiar expression $\hat{g}_F(q) = q^{-1}l^{-1}\exp[-q^2\xi^2/6]\sin ql$.[21] In the limit $\xi \gg l$ we get

$$\hat{g}_F(q) = \exp[-q^2 l_K{}^2/6]\Big\{1 + \frac{1}{2}u(1 + 2P_2(\cos\gamma) + 18q^{-2}l_K{}^{-2}P_2(\cos\gamma))\Big\} - \frac{9}{2\sqrt{6}}uq^{-3}l_K{}^{-3}\sqrt{6\pi}P_2(\cos\gamma)\,\mathrm{erf}(ql_K) \quad (27)$$

which in the absence of the field leads to the regular expression of the standard Gaussian model $\hat{g}_F(q) = \exp[-q^2 l_K{}^2/6]$. In this last formula $P_2(\cos\gamma) = {}^1/_2(3\cos^2\gamma - 1)$ is the second Legendre polynomial. In the limit $ql_K \ll 1$ this expression simplifies to

$$\hat{g}_F(q) = 1 + \frac{1}{2}u - \left(\frac{1}{6} + \frac{1}{12}u + \frac{1}{15}uP_2(\cos\gamma)\right)q^2 l_K{}^2 \quad (28)$$

References and Notes

(1) *Processing of Polymers*; Meijer, H. E. H., Ed.; VCH: New York, 1997; Vol. 18.
(2) Gedde, U. W. *Polymer Physics*; Chapman & Hall: London, 1992.
(3) Carrington, S. P.; Odell, J. A. *J. Non-Newtonian Fluid Mech.* **1996**, *67*, 269.
(4) Smith, D. E.; Chu, S. *Science* **1998**, *28*, 1335.
(5) De Gennes, P. G. *J. Chem. Phys.* **1974**, *60*, 5030.
(6) Peterlin, A. *Pure Appl. Chem.* **1966**, *12*, 273.
(7) Peterlin, A. *Adv. Macromol. Chem.* **1968**, *1*, 225.
(8) Dukovski, I.; Muthukumar, M. *J. Chem. Phys.* **2003**, *118*, 6648.
(9) Hu, W.; Frenkel, D.; Mathot, V. B. F. *Macromolecules* **2002**, *35*, 7172.
(10) de Moel, K.; Flikkema, E.; Szleifer, I.; ten Brinke, G. *Europhys. Lett.* **1998**, *42*, 407.
(11) Flory, P. J. *Proc. R. Soc. London, Ser. A* **1956**, *234*, 60.
(12) Meyer, H.; Müller-Plathe, F. M *Macromolecules* **2002**, *35*, 1241.
(13) Zubarev, A. Yu. *Colloid J.* **1996**, *58*, 189.
(14) Thirumalai, D. *J. Chem. Phys.* **1986**, *84*, 5869.
(15) Khokhlov, A. R.; Semenov, A. N. *Macromolecules* **1982**, *15*, 1272.
(16) Ziabicki, A.; Jarecki, L. *J. Non-Newtonian Fluid Mech.* **2001**, *97*, 31.
(17) Ziabicki, A.; Jarecki, L. *J. Non-Newtonian Fluid Mech.* **2001**, *54*, 269.
(18) Jarecki, L.; Ziabicki, A. *J. Non-Newtonian Fluid Mech.* **1997**, *68*, 43.
(19) Bhattacharjee, S. M.; Fredrickson, G. H.; Helfand, E. *J. Chem. Phys.* **1989**, *90*, 3305.
(20) Kramers, H. A. *J. Chem. Phys.* **1946**, *14*, 415.
(21) Sushko, N.; van der Schoot, P.; Michels, M. A. J. *J. Chem. Phys.* **2001**, *115*, 7744.
(22) Edwards, S. F. *Proc. Phys. Soc.* **1965**, *85*, 613.
(23) van der Schoot, P. *Macromolecules* **2000**, *33*, 8497.
(24) Grosberg, A. Yu.; Khokhlov, A. R. *Statistical Physics of Macromolecules;* AIP Press: New York, 1994.
(25) de Gennes, P.-G. *Scaling Concepts in Polymer Physics;* Cornell University Press: Ithaca, NY, 1979.
(26) Lifshitz, I. M.; Grosberg, A. Yu.; Khokhlov, A. R. *Rev. Mod. Phys.* **1978**, *50*, 3.
(27) Sushko, N.; van der Schoot, P.; Michels, M. A. J. *J. Chem. Phys.* **2003**, *118*, 6098.
(28) Chandler, D.; Singh, Y.; Richardson, D. *J. Chem. Phys.* **1972**, *57*, 1930.
(29) Schweizer, K. S.; Curro, J. G. *Phys. Rev. Lett.* **1987**, *58*, 246.
(30) Laird, B. B.; McCoy, J. D.; Haymet, A. D. J. *J. Chem. Phys.* **1987**, *87*, 5449.
(31) Haymet, A. D. J.; Oxtoby, D. W. *J. Chem. Phys.* **1981**, *74*, 2559.
(32) Frisch, H. L.; Pistoor, N.; Sariban, A.; Binder, K.; Fesjian, S. *J. Chem. Phys.* **1988**, *89*, 5194.
(33) Wang, S.-Q.; Gelbart, W. M. *J. Chem. Phys.* **1989**, *90*, 597.

MA034864R